**doi: 10.12029/gc20220105**

张云,张天福,程先钰,孙立新,程银行,王少轶,王善博,马海林,鲁超. 2022. 鄂尔多斯盆地东北部侏罗纪含铀岩系三维地质结构与铀成矿规律浅析[J]. 中国地质, 49(1): 66-80.

Zhang Yun, Zhang Tianfu, Cheng Xianyu, Sun Lixin, Cheng Yinhang, Wang Shaoyi, Wang Shanbo, Ma Hailin, Lu Chao. 2022. A brief analysis on the three-dimensional geological structure and uranium mineralization of Jurassic uranium-bearing rock series in the northeastern Ordos Basin [J]. Geology in China, 49(1): 66-80(in Chinese with English abstract).

# 鄂尔多斯盆地东北部侏罗纪含铀岩系三维地质结构与铀成矿规律浅析

张云[1,2],张天福[1,2],程先钰[1,2],孙立新[1,2],程银行[1,2],
王少轶[1,2],王善博[1,2],马海林[3],鲁超[4]

(1.中国地质调查局天津地质调查中心,天津 300170;2.中国地质调查局天津地质调查中心非化石能源矿产实验室,天津 300170;3.内蒙古地质调查院,内蒙古 呼和浩特 010000;4.核工业二〇八大队,内蒙古 包头 014000)

**提要:【研究目的】**为了更加直观、准确地揭示鄂尔多斯盆地东北缘侏罗纪含铀岩系直罗组三维空间展布规律,开展铀成矿规律研究和找矿预测工作。**【研究方法】**本文利用首次建立的钻孔—测井综合数据库,精细构建了东胜铀矿集区多尺度、多类型的三维地质模型并实现其可视化功能。**【研究结果及结论】**综合地质建模研究发现本区铀成矿具有以下特征:(1)受直罗组沉积期"北高南低、东高西低"古地貌格局的影响,纳岭沟—大营地区直罗组下段存在区域性沉积相变,由北部呼斯梁—唐公梁古隆起区向西、向南方向,沉积体系由冲积扇—砾质辫状河向砂质辫状河、辫状河三角洲沉积有序转变,大营铀矿化集中产于辫状河向辫状河三角洲沉积过渡部位的分流河道一侧,纳岭沟铀矿化主要产于砾质辫状河之上的砂质辫状河道中;(2)自东部呼斯梁向西部大营地区,直罗组下段铀储层的非均质性增强,具体表现为砂体厚度明显减薄、含砂率降低、泥岩层数量和厚度均显著增加、内部开始发育薄层煤线。这种组合的出现在大营西侧形成了规模较大的横向泥质隔挡层和垂向还原层,在后期成矿过程中极大地抑制了层间氧化带向西推进的速率和里程,从而在大营一带形成稳定的层间氧化带前锋线和持续的铀矿化;(3)矿床尺度的三维地质建模显示,大营弧形展布的铀矿化体与东部相邻的纳岭沟—塔然高勒铀矿化几乎相连,且两矿床之间的伽马三维属性模块亦有较强的放射性异常显示,指示着大营与纳岭沟之间的塔然高勒—乌定布拉格地区具有很好的找矿潜力。

**关 键 词:**侏罗纪;砂岩型铀矿;直罗组;三维建模;铀矿勘查工程;东胜;鄂尔多斯盆地

**创 新 点:**利用煤-铀钻孔数据库"大数据"优势,开展多尺度、多类型三维地质建模,更加直观、客观、准确地揭示了鄂尔多斯盆地北缘含铀岩系的空间展布规律;基于对三维地质模型的信息挖掘,开展了铀成矿规律研究和找矿预测工作。

**中图分类号:**P619.108 **文献标志码:**A **文章编号:**1000-3657(2022)01-0066-15

# A brief analysis on the three-dimensional geological structure and uranium mineralization of Jurassic uranium-bearing rock series in the northeastern Ordos Basin

**收稿日期:**2019-11-24;**改回日期:**2020-05-08

**基金项目:**国家自然科学基金重点支持项目(92162212),中国地质调查局项目(DD20190121)和国家重点研发计划项目(2018YFC0604200)联合资助。

**作者简介:**张云,男,1991年生,工程师,从事区域地质矿产调查与研究工作;E-mail:571938243@qq.com。

**通讯作者:**张天福,男,1985年生,高级工程师,从事地质矿产调查与研究工作;E-mail:tianfuzhang85@163.com。

ZHANG Yun[1,2], ZHANG Tianfu[1,2], CHENG Xianyu[1,2], SUN Lixin[1,2], CHENG Yinhang[1,2], WANG Shaoyi[1,2], WANG Shanbo[1,2], MA Hailin[3], LU Chao[4]

(1. *Tianjin Center, China Geological Survey, Tianjin* 300170*, China;* 2. *Key Laboratory of Uranium Geology, China Geological Survey, Tianjin* 300170*, China;* 3. *Inner Mongolia Institute of geological survey, Hohhot* 010010, *Inner Mongolia, China;* 4. *No. 208 Geological Party, CNNC, Baotou* 014010, *Inner Mongolia, China*)

**Abstract**: This paper is the result of mineral exploration engineering.

**[Objective]**In order to more intuitively and accurately reveal the three-dimensional spatial distribution of the Jurassic uranium-bearing rock series (the Zhiluo Formation) in the northeastern margin of the Ordos Basin, the research on the uranium metallogenic characteristics and the prospecting and prediction work were carried out.**[Methods]**In this paper, we used the first established comprehensive database consists of drills, logging to construct the three-dimensional geological models with different scales and types and realized its visualization function in the Dongsheng uranium area. **[Results and Conclusions]**Comprehensive geological modeling shows that uranium mineralization in this area has the following characteristics: (1) Under the influence of the paleogeomorphic pattern of "high in the north and low in the south, high in the east and low in the west" during the depositional period of the Zhiluo Formation, there was a regional sedimentary facies transition in the lower section of the Zhiluo Formation in the Nalinggou-Daying area. From the northern Husliang-Tanggongliang paleo-uplift area to the west and south, the sedimentary system gradually changed from alluvial fan-gravel braided river to sandy braided river and braided river delta deposition. Uranium mineralization in Daying area is concentrated in the distributary channel of braided river to braided river delta, while uranium mineralization in Nalinggou is mainly in the sandy braided river which was above the gravel braided river; (2) The heterogeneity of uranium reservoir in the lower member of Zhiluo Formation increased from Husiliang in the east to Daying area in the west, which is manifested as a significant reduction in the thickness of the sand body, a decrease in the sand content ratio, a significant increase in the number and thickness of mudstone layers, and the inner coal-line began to develop. The occurrence of above combination formed a large-scale lateral argillaceous barrier layer and vertical reduction layer on the west side of Daying, which greatly inhibited the westward propulsion rate and distance of the interlayer oxidation zone. Therefore, a stable front line of interlayer oxidation zone and continuous uranium mineralization are formed in the Daying area; (3) By the three-dimensional geological modeling of ore deposits, it can be found that the arc-shaped uranium mineralization body in Daying area is almost connected with the uranium mineralization in Nalinggou-Tanggongliang. Meanwhile, the three-dimensional $\gamma$ property model between the two deposits also shows strong radioactive, which indicate that the Tarangaole-Wudingbulage area between Daying and Nalingou diposits has a good prospecting potential.

**Key words:** Jurassic; sandstone-type uranium; Zhiluo Formation; three-dimensional modeling; uranium exploration engineering; Dongsheng; Ordos Basin

**Highlights**: Using the advantage of "big data" of coal-uranium drill database, multi-scale and multi-type 3D geological modeling was carried out, which revealed the spatial distribution regularities of the uranium bearing rock series in the northern margin of Ordos Basin more intuitively and accurately. Based on the information mining of the 3D geological model, the research of uranium metallogenic regularity and prospecting prediction were carried out.

**About the first author:** ZHANG Yun, male, born in 1991, engineer, engaged in regional geology and mineral survey; E-mail: 571938243@qq.com

**About the corresponding author:** ZHANG Tianfu, male, born in 1985, senior engineer, engaged in geological and mineral survey; E-mail: tianfuzhang85@163.com.

**Fund support:** Supported by National Science Foundation of China(No.92162212), the project of China Geological Survey (No. DD20190121) and National Key R&D Program of China (No.2018YFC0604200) from the Ministry of Science and Technology.

## 1 引　言

近年来,以平面图和剖面图为主的传统地质信息的表达难以满足大数据信息化趋势的迫切需求,三维地质建模及可视化的研究已引起诸多领域的广泛重视,逐渐成为诸多国家“玻璃地球”战略和地

质大数据多源异构数据整合的支撑技术之一(陈应军和严加永,2014;吴冲龙等,2015)。国内外学者对三维地质建模的理论与技术进行了不懈的探索,如煤田、油田、矿山勘探部门利用大量钻孔岩心测井资料、地球物理资料,结合计算机成图技术对三维地质结构的表达进行了很好的尝试(Guiziou et al., 1996; Courriox et al., 2001; Jachens et al., 2001; Malolepszy, 2005; Mallet, 2008;焦养泉等,2006;2018;崔廷主和马学萍,2010;毛先成等,2010;陈超和陈广峰,2012;邵燕林等,2012);以MapGIS、DeepInsight及Creatar等国产软件为平台,针对造山带的"三维地质填图"、油气勘探、固体矿床勘探及城市地质与城市区地下空间管理方面的应用也已初见成效(朱良峰等,2004;郁军建等,2015;李青元等,2016)。

相对于传统的二维地质数据表达方法,三维模型能够完整、准确地表达各种地质现象,直观地再现各地质体的空间展布及其相互关系,挖掘隐含的地质信息,最大限度地提高地质分析的直观性和准确性,方便勘探工程决策和自动制图。其中,钻孔又是获取三维地质信息的最直观和精确的手段。近10年来,随着鄂尔多斯盆地北缘东胜地区勘查程度的日益提高,已积累有海量的煤-油-铀钻孔、测井及地震资料,这为本区含铀岩系三维模型的构建提供了可靠的数据支撑。尤其是纳岭沟—大营铀矿集区,勘查井网密度高,钻孔资料丰富,已具备开展井下铀储层三维地质建模的基本条件(张天福等,2016,2019,2020;俞礽安等,2020)。为此,本文从三维地质建模的角度出发,首次建立了中国北方最大的煤-铀钻孔数据库,该数据库涵盖了近4500余口钻孔、测井数据及110 km二维地震数据,涉及面积近5000 km$^2$,并且具有较高的精度和网度。基于该数据库,本文通过构建大营—纳岭沟矿集区含铀岩系不同尺度、不同类型的三维可视化地质模型,实现模型及各地质体在三维空间的任意组合、旋转及任意方位的切割显示,对本区开展成矿规律研究和服务找矿预测工作均具有重要的实际应用价值。

## 2 区域地质背景

鄂尔多斯盆地是中国重要的油气、煤、铀等多种能源共存产出的大型中、新生代陆相盆地之一(刘池洋等,2006;金若时等,2017;苗培森等,2017;Jin et al., 2019, 2020)。在稳定的华北克拉通结晶基底之上,盆地内记录了早古生代碳酸盐台地相沉积、晚古生代海陆交互相沉积和中生代内陆湖盆相沉积等厚达万米的沉积地层。盆地边缘断裂、褶皱较发育,盆内构造相对简单,主要以隆起、坳陷、宽缓褶皱为主(杨俊杰和裴锡古,1996)(图1 a)。鄂尔多斯盆地中生代侏罗系陆相沉积是研究区内煤、铀和其他能源矿产主要赋存场所(Li et al., 1995;刘晓雪等,2016;陈印等,2017;俞礽安等,2020)。研究区位于盆地东北缘伊蒙隆起区,区内岩浆活动不发育,出露地层以中、新生界为主。其中三叠系、侏罗系多分布盆地周缘,露头分布区主要见于鄂尔多斯盆地东北缘东胜、准格尔一带(李思田等,1990;Li et al., 1995),白垩系多分布在盆地中部(图1 b)。中—下侏罗统延安组($J_{1-2}y$)及中侏罗统直罗组($J_2z$)发育最为齐全,其地层序列相对完整,且分布广泛,分别为盆内主要的含煤和含铀岩系(张天福等,2018)(图1 c)。

## 3 钻孔数据库的建立

钻孔数据是三维地质建模的基础和前提,其精度和网度直接影响到地质模型的准确性和可靠性。东胜煤田区及铀矿区积累了海量的钻孔、测井资料,但钻孔资料具有多源、异构(多来源、多维度、多类型)的特点。为了便于钻孔资料的统一管理及二次开发利用,笔者参照周小希等(2016)所设计的25张数据表(图2),按照统一的标准和要求全面采集了3200余口钻孔资料属性数据,通过整理、数据类型转换、录入和集成,首次建成了中国北方产铀盆地最大的综合钻孔数据库,这为三维地质建模及铀成矿规律研究提供强大的数据支持。

## 4 三维地质模型

本着从框架到内部建筑结构和内部属性这一原则,首先建立侏罗系延安组—直罗组格架模型,其次建立包含砂体沉积单元的层模型,最后在储层砂体单元骨架内建立储层属性参数模型。以层序地层学为重要依据,通过对鄂尔多斯盆地北部侏罗纪含煤含铀岩系露头剖面的解剖和多井对比工作,将含煤岩系延安组精细解剖为3个沉积单元,包含

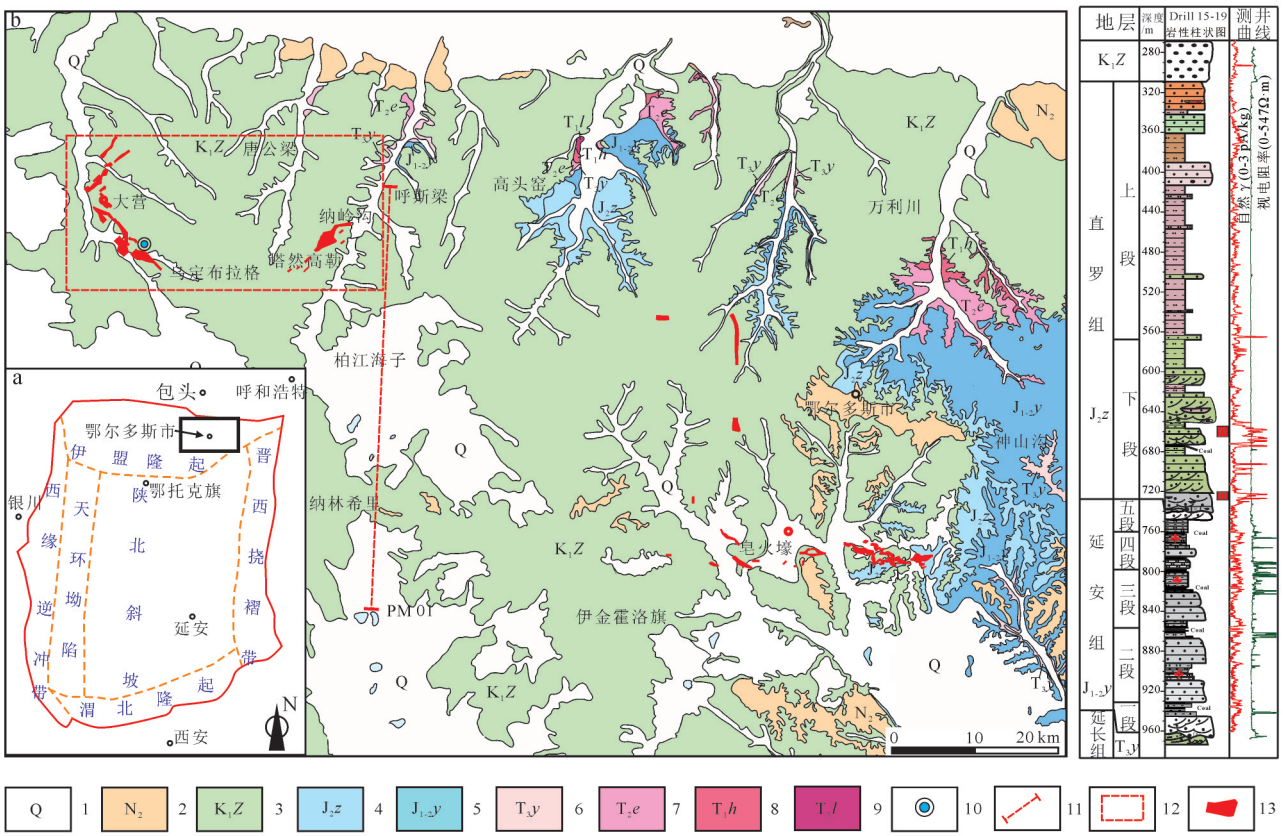


图1 鄂尔多斯盆地东北缘构造位置图、地质简图(a,b)及钻孔柱状图(c)(a,据杨俊杰和裴锡古,1996修改)

1—第四系;2—新近系上新统;3—下白垩统志丹群;4—中侏罗统直罗组;5—中—下侏罗统延安组;6—上三叠统延长组;7—中三叠统二马营组;8—下三叠统和尚沟组;9—下三叠统刘家沟组;10—钻孔位置;11—文中剖面PM01所在位置;12—研究区位置;13—砂岩铀矿床

Fig.1 Geotectonic location and geological schematic map of Dongsheng district on the northeastern margin of Ordos Basin (a,b) and the histogram of well 15−19 in Daying ore deposit( a ,modified from Yang Junjie and Pei Xigu, 1996)

1−Quaternary; 2−Pliocene; 3−Lower Cretaceous Zhidan Group; 4−Middle Jurassic Zhiluo Formation; 5−Lower- Middle Jurassic Yan'an Formation; 6−Upper Triassic Yanchang Formation; 7−Middle Triassic Er'maying Formation; 8−Lower Triassic Heshanggou Formation; 9−Lower Triassic Liujiagou Formation; 10−Location of drilling; 11−Location of PM01 stratigraphic correlation profiles; 12−Location of study area; 13−Sandstone-type uranium deposits

延安组一岩段、二岩段和三岩段;由于直罗组下段的上亚段对下亚段冲刷严重,导致上、下亚段间普遍缺失1煤组,仅在局部区域发育(如大营地区)(Jiao et al., 2016; 鲁超等,2018),所以本次建模过程中将直罗组下段砂岩作为一个复合铀储层砂体对待,按照上述思路将直罗组解剖为2个沉积单元,即直罗组下段和直罗组上段。针对以上5个沉积单元分别进行了古地貌恢复及三维建模、储层砂体建模、岩性粒度及铀矿化体属性建模。本次建模重点为含铀岩系直罗组,从矿床中尺度和区域大尺度,分层次、循序渐进地系统开展三维建模工作;此次从钻孔数据库中筛选出参与建模的钻孔数量共计为3250口,其中大营—塔然高勒—纳岭沟矿区钻孔控制网度为200 m×200 m,矿区外围钻孔控制网度为2 km×2 km。当然,钻孔间距再小也避免不了二维空间分辨率的差异,即钻孔具有丰富的、连续的垂向信息,而缺少横向井间信息(焦养泉等,2018)。所以本次在井下三维建模的同时,充分借鉴东胜神山沟天然的野外露头"三维模型",将露头区直罗组下段清晰的地层、砂体结构特征及辫状分流河道三维展布规律拓展应用于地下三维建模,并辅以大量地层−砂体对比剖面、大尺度横纵切面、等时切面等二维图件的约束,尽量减少人为预测性,从而保证三维模型的可靠性、真实性。限于篇幅有限,本次具体的建模流程可参照向中林等(2009),在此不再赘述。

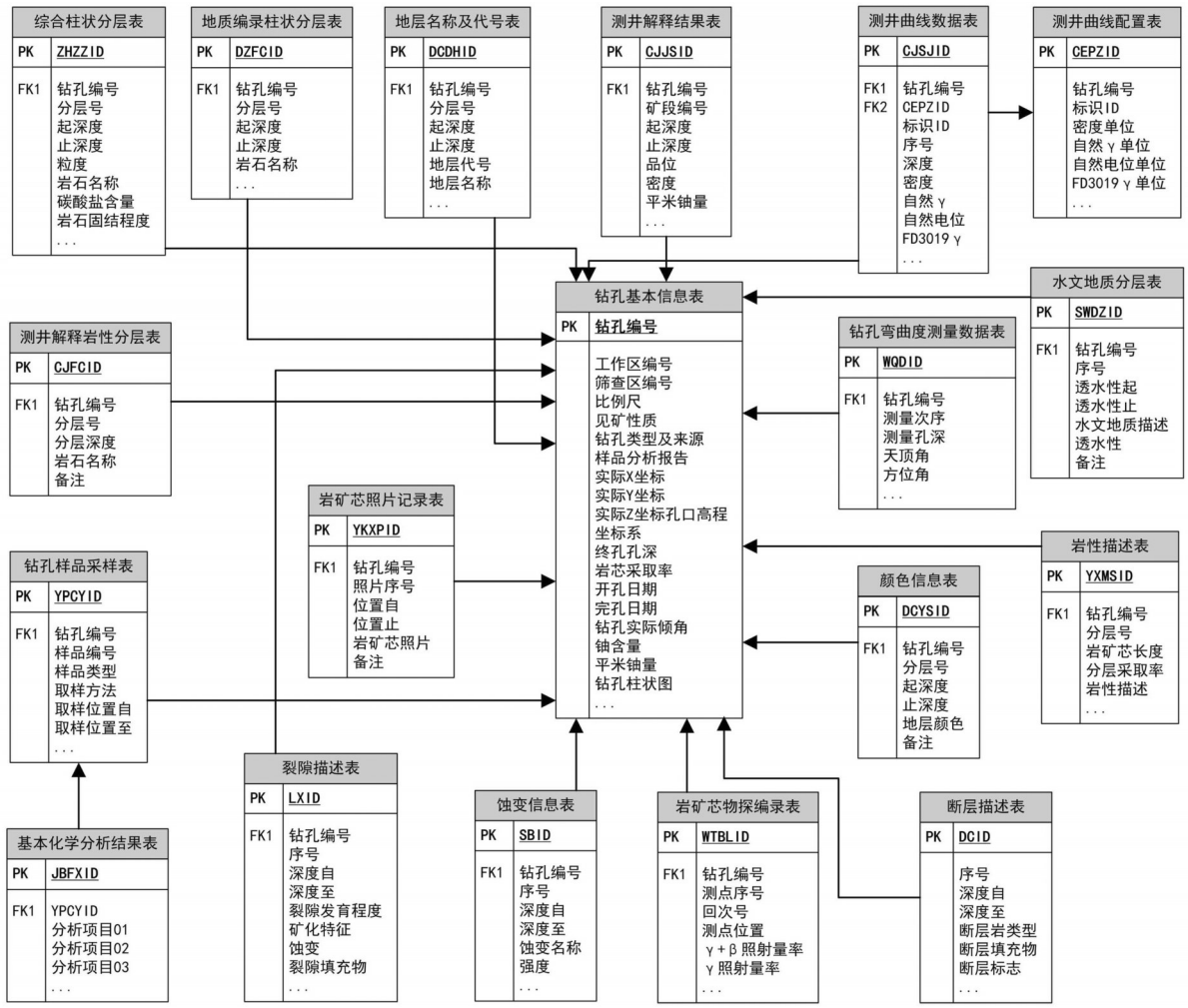


图2 钻孔属性数据表逻辑结构图(据周小希等,2016修改)

Fig.2 Logical structure diagram of drills properties data sheet(modified from Zhou Xiaoxi et al., 2016)

### 4.1 古地貌恢复及古地貌三维模型

古地貌对沉积体系与铀储层分布具有明显的控制作用通过恢复古地貌三维结构,有助于揭示物源与沉积体系的时空配置关系,从而进一步揭示沉积相和优质铀储层的分布规律(焦养泉等,2012,2015;Jiao et al., 2016; 张云等,2016)。目前常见的古地貌恢复方法主要有印模法、沉积学法、残余厚度法、地球物理法和层序地层学法(王鑫等,2013)。考虑到研究区具备大量均匀分布的钻孔和二维地震数据作为支撑,本文首先选取层序地层学法和残余厚度法建立地质模型框架,辅以地球物理法进行修改完善,然后以工作站Gxplorer软件为平台,利用其三维可视化模块将各时期古地貌转化为三维可视化显示,从而做到直观真实,其具体流程和技术路线方法可参照王鑫等(2013)。

东胜地区延安组—直罗组下段沉积前的古地貌三维形态显示:研究区北部呼斯梁—唐公梁—高头窑及东部万立川—神山沟—西召为古隆起区(图3),具有"北高南低,东高西低"的古地貌特征,主要包括古隆起、斜坡和古坳陷3种古地貌单元。由图3可以看出,本区已发现的3处铀矿床及柴登、青达门等其他几处铀矿化点均集中分布于古隆起向古坳陷过渡部位的斜坡地带(图3)。

古隆起:研究区内地形处于相对较高的地貌单元,主要分布于研究区东部和北部。在古隆起区,直罗组上段部分遭受剥蚀,甚至缺失,下段沉积厚度亦相对较薄,沉积物粒度相对较粗,如更加靠近东部隆起区的皂火壕铀矿床(图3),其直罗组上段

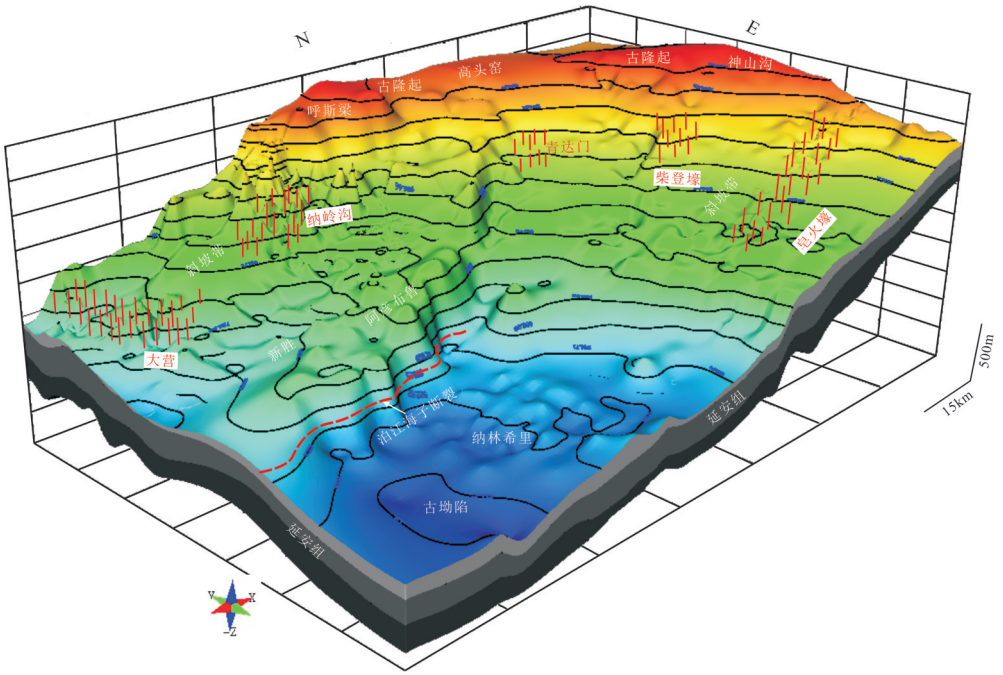


图3 鄂尔多斯盆地东北缘东胜地区直罗组沉积前古地貌三维模型

（矿区外围钻孔控制网度平均为2 km×2 km，矿区钻孔网度为200 m×200 m，局部可达100 m×100 m；模型中只显示了已发现铀矿床及矿化点的部分钻孔）

Fig. 3 Three− dimensional model of paleogeomorphology before the deposition of Zhiluo Formation in the Dongsheng district, northeastern margin of Ordos Basin

(The average borehole control network around the mining area is 2 km × 2 km, and the drilling network in the mining area is 200 m × 200 m, locally up to 100 m × 100 m; Model only shows some of the drill holes where uranium deposits and mineralisation have been discovered)

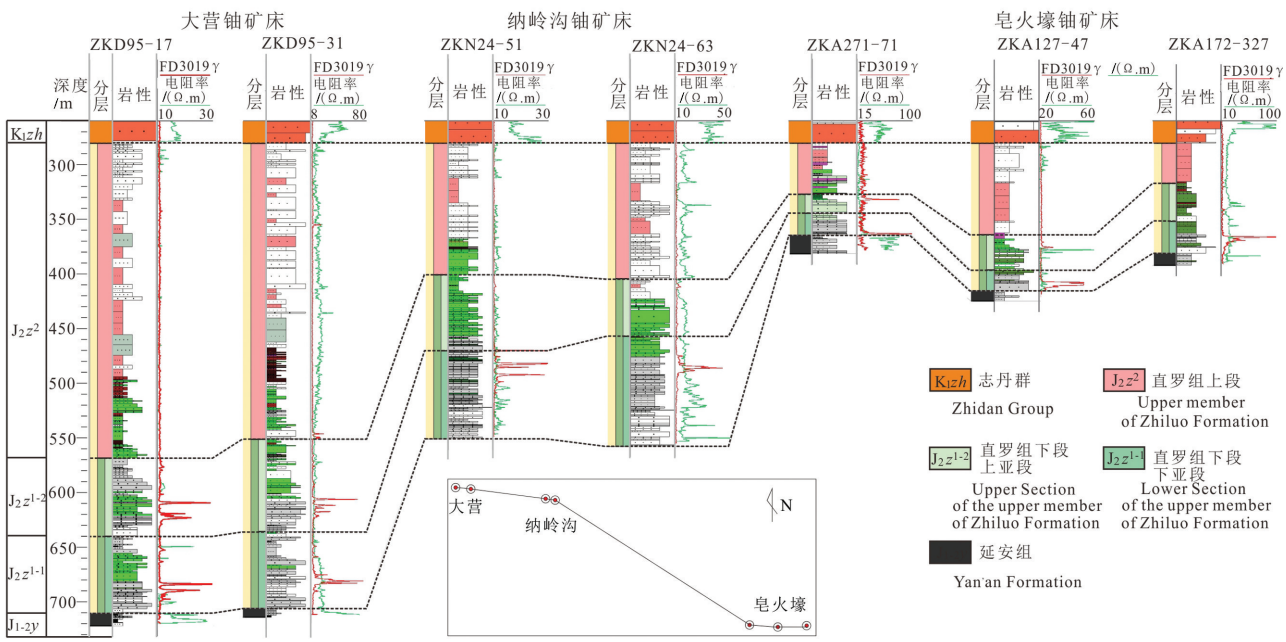


图4 鄂尔多斯盆地皂火壕—纳岭沟—大营铀矿床直罗组地层对比剖面

Fig. 4 Stratigraphic correlation section of Zhiluo Formation in Zaohuohao−Nalinggou−Daying uranium deposits, Ordos Basin

残留厚度仅40~80 m,下段沉积厚度为40~60 m(图4)。

斜坡带:为古隆起和古坳陷区的过渡地带,东部斜坡较陡,坡降为10~12 m/km,西北部斜坡相对较为宽缓,坡降为2~10 m/km。位于西北部斜坡带上的纳岭沟铀矿床直罗组上段残留厚度50~120 m,下段沉积厚度150~180 m;大营铀矿床位于西北部斜坡带上更加靠近坳陷区的位置,其直罗组上段保留相对完整,厚度可达200~280 m,直罗组下段沉积厚度也相对较大,可达180~220 m(图4)。

古坳陷:研究区内地形处于相对较低的地貌单元,主要分布于南部纳林希里一带(图3)。古地貌三维模型显示,沿杭锦旗—新胜—泊江海子一带发育一条显著的近东西向泊江海子大断裂,其南北两侧高程落差可达200 m以上(图3)。多条南北向大尺度的连井剖面均显示,断折带南部直罗组上段的泥岩段与北部直罗组下段的砂岩段近于同一标高范围内,从而形成一条近东西向延伸的区域性物性隔挡层(图5)。

### 4.2 铀储层粒度三维属性模型

由直罗组下段粒度三维属性模型可以看出,由呼斯梁—高头窑隆起边部向西、向南斜坡及坳陷区,直罗组下段发育一套完整的冲积扇—辫状河—辫状河三角洲沉积体系组合(图6)。砂体纵切剖面显示,直罗组下段辫状河道砂体呈板状,在三维空间分布比较稳定,且规模大、连续性好(图6,图7)。靠近古隆起(如呼斯梁—纳岭沟地区),直罗组下段下部砂体叠置方式以切叠式为主,由于多期河道切叠较重,河道间细粒沉积物不发育,表现为复合砂体特征,在三维模型上显示为"泛连通厚"(图6)。该地区的辫状河道砂体或主干辫状分流河道砂体通常具有较好的连通性和均质性,是成矿流体的快速运移和输导通道,也是层间氧化带的有利发育空间。

靠近坳陷区(如大营地区),直罗组沉积表现为辫状河沉积体系向辫状河三角洲沉积体系过渡特征(图6)。该地区直罗组下段中部开始发育1~2层薄煤线,明显可以划分出2个短期旋回组合,即直罗组下段下亚段和直罗组下段上亚段,垂向序列具有先倒粒序、后正粒序的特征,表现出辫状河三角洲沉积体系特点。大量纵向砂体剖面显示,该地区直罗组下段砂体开始频繁分岔,河道单元之间泥质隔挡层开始增多(图7)。大营西部沉积相的转变和大

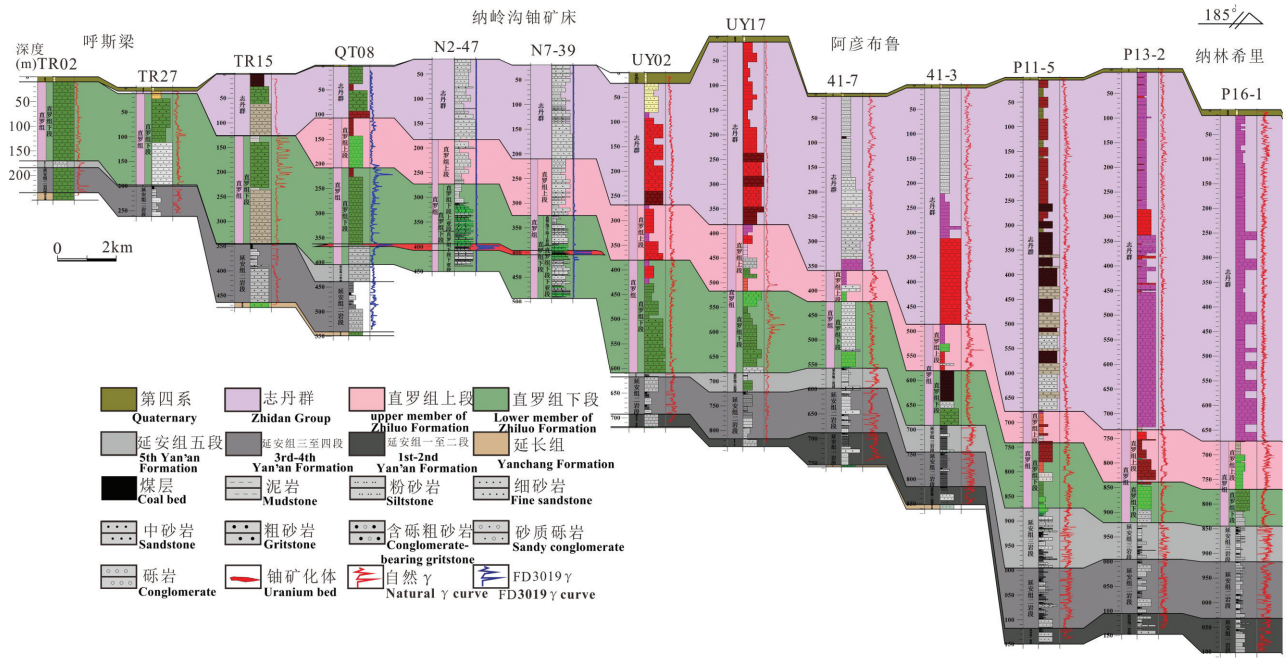


图5 鄂尔多斯盆地呼斯梁—纳林希里地区延安组—志丹群地层对比剖面(PM01)

Fig. 5 Stratigraphic correlation section between Yan'an Formation and Zhidan group from Husiliang area to Nalinxili area, Ordos Basin

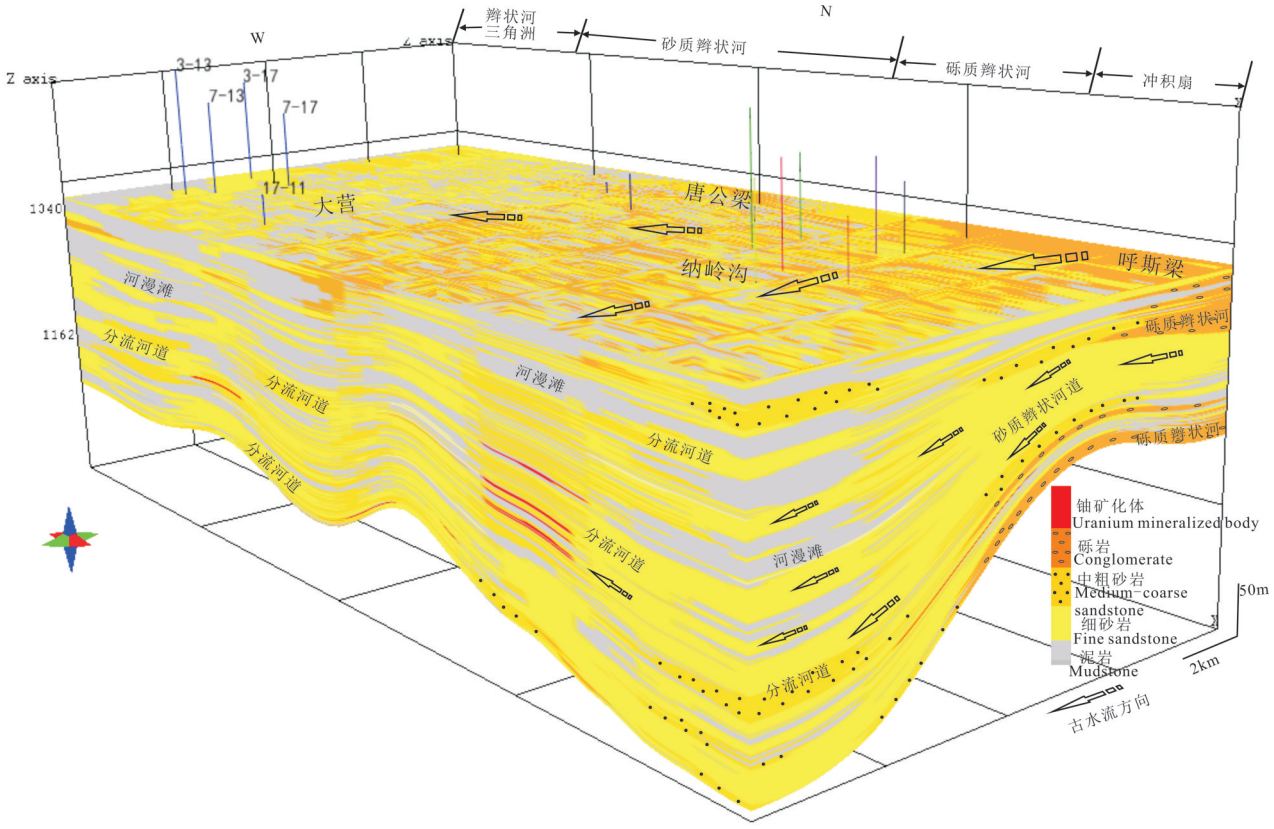


图6 大营—纳岭沟矿区直罗组下段岩性粒度三维属性模型与铀矿化关系

Fig. 6 The relationship between the three-dimensional model of particle size attribute and uranium mineralization in the lower member of Zhiluo Formation in the Daying-Nalinggou uranium concentration area

量薄煤层及泥质隔挡层的出现在很大程度上限定了层间氧化带向西推进的里程,使得铀矿化多集中产于大营及大营以东地区的辫状分流河道之中(图6,图7)。

等时横切平面上,直罗组下段自下而上的不同层位中,沉积物粒度也有规律可循,随着层位的升高,沉积物粒度整体变细(图8)。自下而上铀储层中泥质隔挡层无论是发育层数还是累积厚度均有显著增加趋势(图8a~c),反映铀储层砂体非均质性逐渐增强。这种变化符合辫状分流河道的固有演化周期(正韵律特征),取决于沉积期古水动力的周期演化。此外,各层位等时平面图显示,隔挡层具有不明显的向北东方向迁移的特征(图8a~c)。

### 4.3 铀矿化体三维属性模型

为了更好地揭示岩性粒度与铀矿化空间耦合关系,笔者将纳岭沟—大营地区直罗组下段粒度三维属性模型与铀矿化体三维属性模型进行套合(图9)。由图8和图9可以看出,在纳岭沟—塔然高勒—乌定布拉格一带,存在着一条近于NWW向、由于相变而致且具有穿时性质的岩性(砂岩/砾岩)转换带,而且自下而上砾岩分布具有明显向北东方向萎缩趋势(图8),铀矿化主要分布于南侧的砂岩分布区,其北侧唐公梁—呼斯梁一带的砾岩区(冲积扇区)铀矿化则极为少见。前人研究发现,已发现的皂火壕、纳岭沟及大营铀矿床中具有工业意义的铀矿体绝大多数是板状的,即用工业指标圈定的"富铀"铀矿体是板状的(焦养泉等,2018)。但是,从大量连井剖面及本次所构建的铀矿化体(即包含了铀异常、低品位和高品位地质体)三维属性模型来看,大营铀矿区明显具有两层铀矿化,类似于典型砂岩型铀矿的"卷头"部位,且表现出下翼(下层)矿化强度整体大于上翼(上层),相比而言,纳岭沟和皂火壕铀矿床只发育"下翼"铀矿化体(图4,图9)。大营弧形展布的铀矿化体与东部相邻的纳岭沟—塔然高勒铀矿化几乎相连、相通(图9,图10,图11c),且铀矿化体三维属性模型显示两矿床之间亦存在较

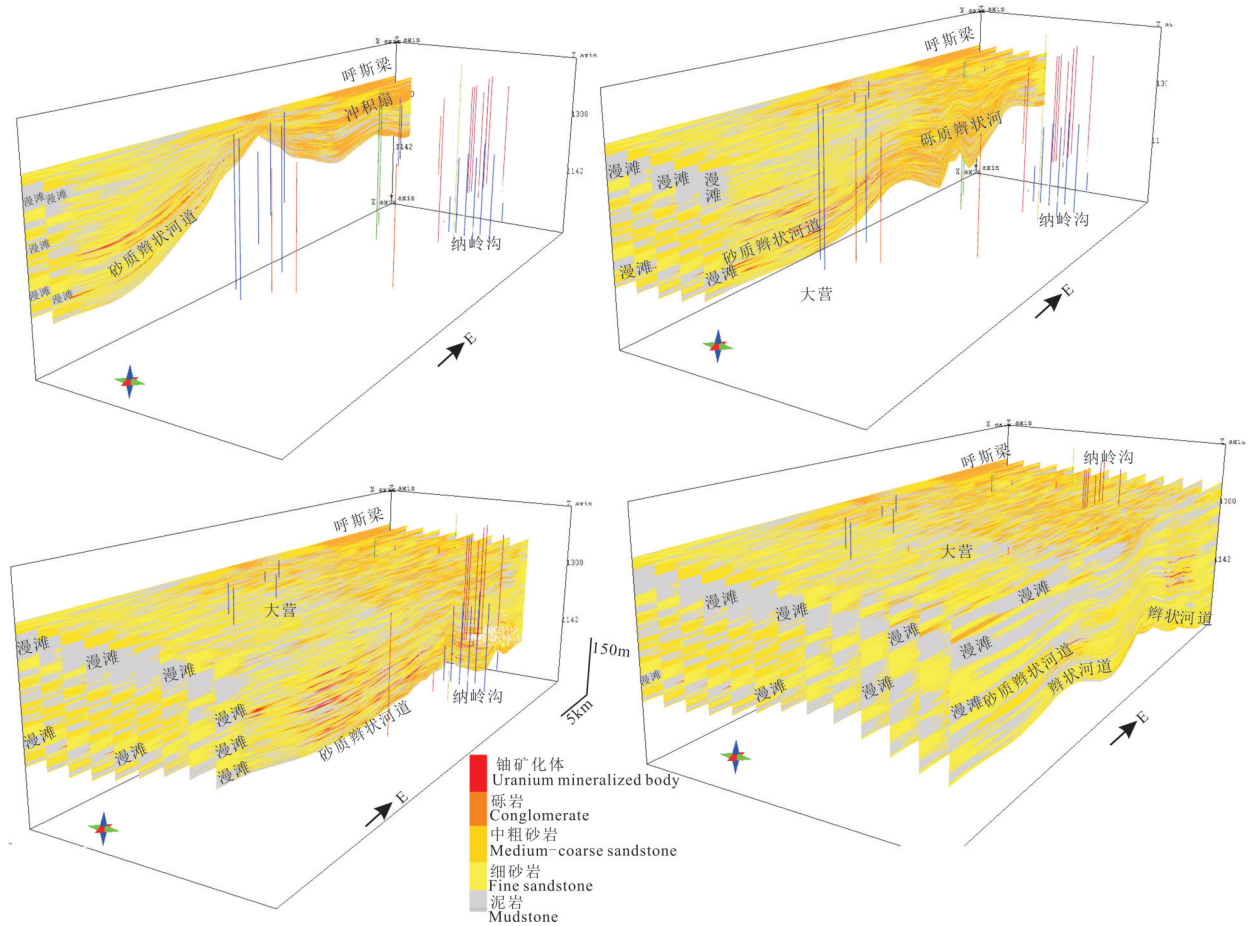


图7 大营—纳岭沟矿区直罗组下段东西向系列纵切剖面

Fig. 7 A series of longitudinal sections of the lower member of Zhiluo Formation in Daying- Nalinggou area

强的放射性异常(图9),指示着大营与纳岭沟矿床之间的塔然高勒至乌定布拉格一带具有相似的成矿地质条件及很好的找矿潜力。本地区这种铀矿化的展布形态在一定程度上可以近似代表层间氧化带前锋线的大致走向,暗示着本区成矿流体场很可能为北东—南西向(图11c)。

## 5 含铀岩系三维地质结构与铀成矿规律

综合上述研究不难发现,研究区直罗组沉积期的“东高西低,北高南低”的古地貌格局不仅控制了沉积体系和沉积相的空间分布,而且这种隆坳格局还间接控制了潜在铀储层及其隔水层的三维空间配置。本区粒度三维模型揭示了北部高头窑—呼斯梁一带为盆地边缘相,发育一套厚近200 m的冲积扇-砾质辫状河等冲积体系,向南、向西逐渐过渡为砂质辫状河、辫状河三角洲沉积体系,指示着古水流方向整体为自北向南,并发育自北东向南西的分流河道(图10,图11a)。北部唐公梁—呼斯梁—高头窑隆起区的铀储层剥蚀暴露地表而沟通了与蚀源区的通道,而南部的泊江海子断裂则可能充当了区域含矿流场的泄水通道,两者共同构成了完整的补—径—排成矿流体系统。

大营—纳岭沟地区铀矿化的分布格局与铀储层砂体非均质性存在着密不可分的关联性:靠近西部大营地区,直罗组下段铀储层砂体的非均质性明显增强,具体表现为砂体厚度明显减薄、含砂率降低(图11a),泥岩层数量和厚度均显著增多,并且直罗组下段内部开始发育有薄煤层,这种组合在大营西侧形成了规模较大的横向泥质隔挡层和垂向还原层(图11b,X1剖面)。受古地貌影响,本区成矿流体由北部呈扇形沿直罗组下段铀储层渗流,在大营西侧遇到辫状河三角洲相泥质隔挡层和薄煤层,极

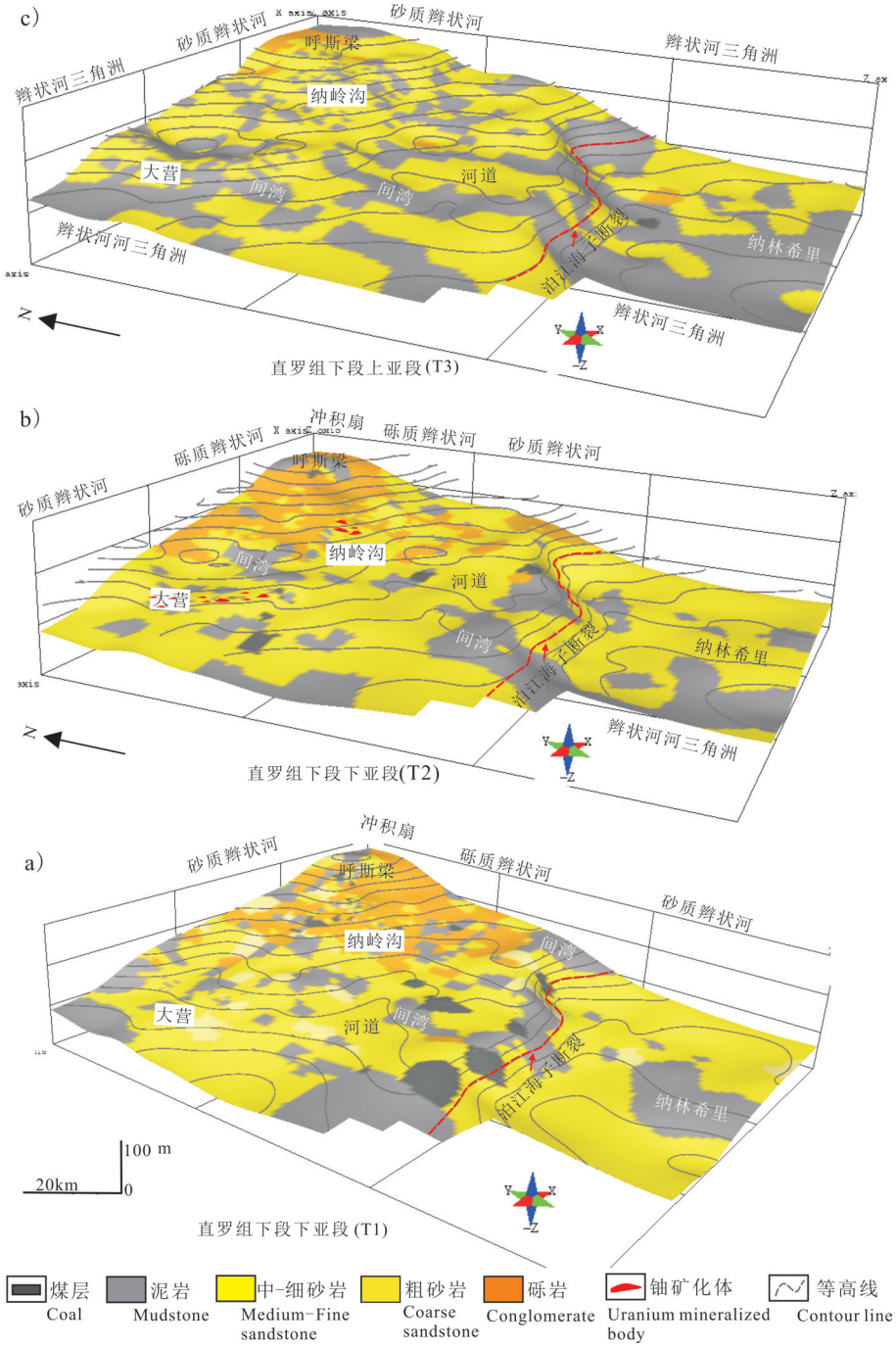


图8 大营—纳岭沟—纳林希里地区直罗组下段粒度三维属性模型不同层位的等时横切平面

Fig. 8 Isochronous crosscutting planes of different layers in the lower member of Zhiluo Formation in Daying- Nalinggou-Nalinxili area

大地抑制了成矿流体向西侧向运移,从而在大营一带形成稳定的层间氧化带前锋线和近于南北向弧形展布的铀矿化体(图11c)。该弧形展布的南端铀矿化体向东部延伸,几乎与塔然高勒、纳岭沟一带的铀矿化体相连、相通,这种铀矿化的三维空间展布几乎勾勒出了本地区氧化带前锋线大致走向,指示着成矿期的含矿流体场整体为自北东向南和南西方向(图11c)。岩性粒度和铀矿化体三维属性综合模型亦显示,本地区成矿流体场和铀储层(直罗组)沉积期古水流方向具有较好的一致性(图11a、

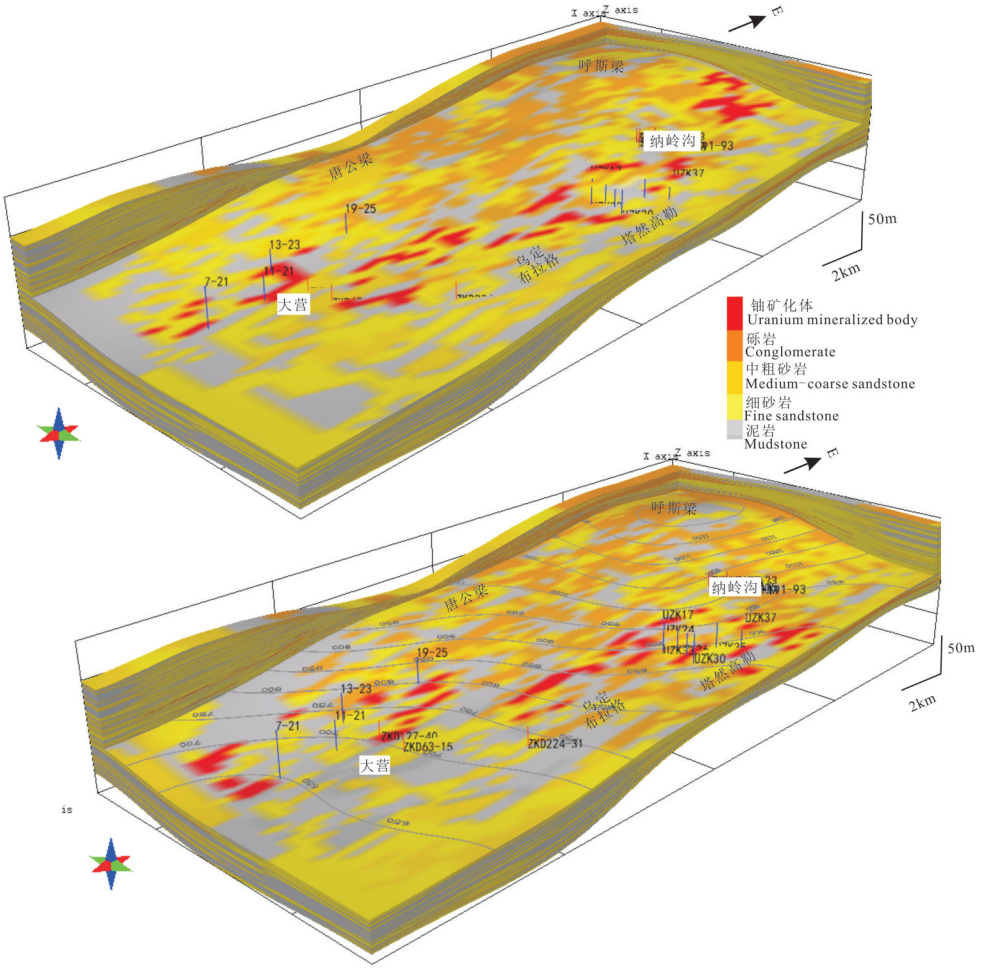


图9 大营—纳岭沟矿区直罗组下段相邻层位铀矿化与岩性粒度的三维展布

Fig. 9 Three-dimensional distribution of uranium mineralization and lithologic-particle size from adjacent strata in the lower member of Zhiluo Formation in Daying- Nalinggou area

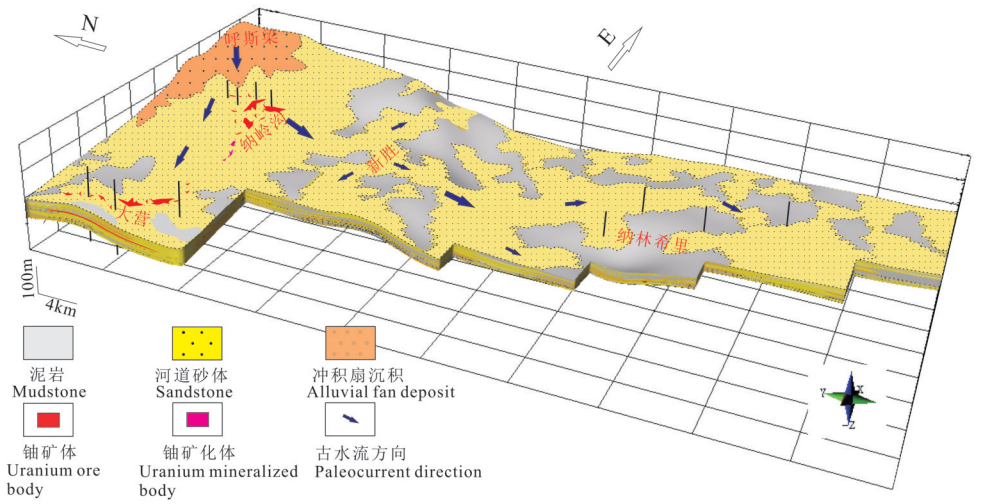


图10 大营—纳岭沟—纳林希里地区直罗组下段骨架砂体三维空间展布及古水流方向

Fig. 10 Three-dimensional spatial distribution of skeleton sand bodies of lower member of Zhiluo Formation and the paleocurrent direction in Daying-Nalinggou-Nalinxili area

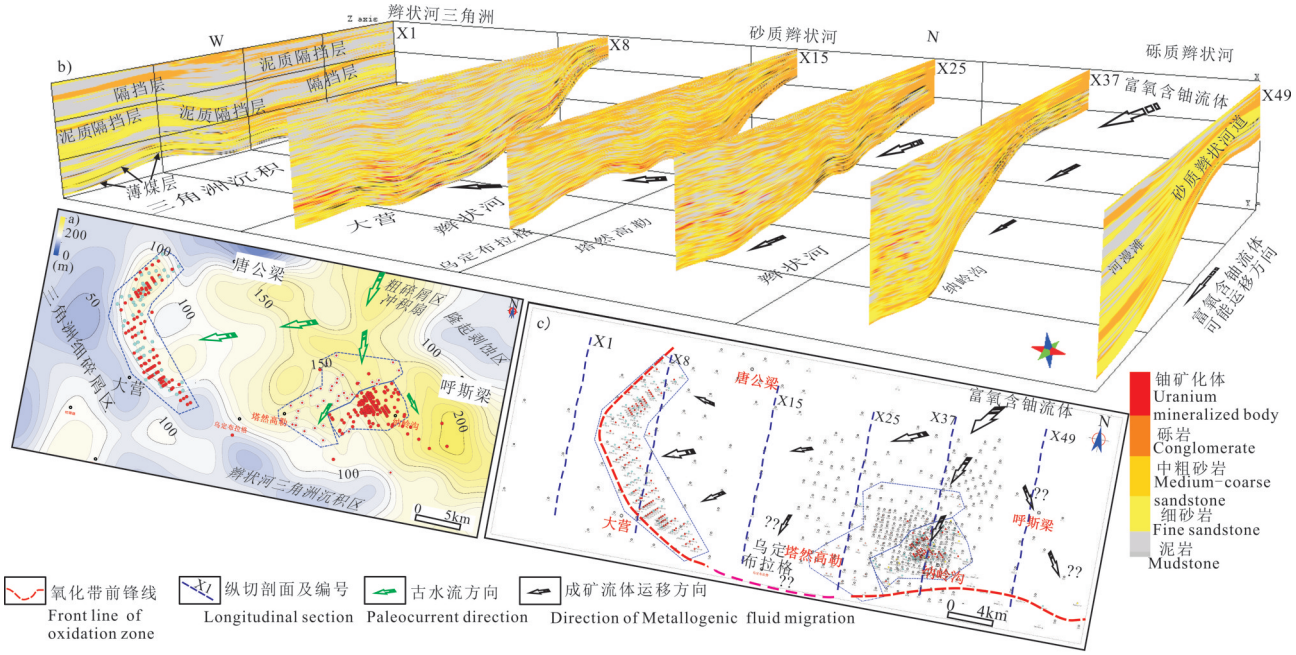


图11 大营—纳岭沟矿区直罗组下段砂体等厚图(a)、骨架砂体南北向切面(b)及成矿流体场示意图(c)

Fig. 11 Contour map of sand body (a), North− South section of skeleton sand body (b) and schematic diagram of ore− forming fluid field (c) in the lower member of Zhiluo Formation in Daying− Nalinggou area

c),这很可能是造就大营、纳岭沟大型—超大型铀矿床的主控因素。

## 6 结　论

(1)直罗组沉积期古地貌三维模型显示,东胜地区整体显示为“北高南低、东高西低”,受该地貌格局影响,纳岭沟—大营地区直罗组下段存在区域性沉积相变:由北部呼斯梁—唐公梁一带的古隆起区向西、向南方向延伸,沉积体系由冲积扇—砾质辫状河沉积向砂质辫状河、辫状河三角洲沉积有序转变,大营铀矿化集中产于辫状河向辫状河三角洲沉积过渡部位的分流河道一侧,纳岭沟铀矿化主要产于砾质辫状河之上的砂质辫状河道之中。

(2)自东部呼斯梁一带向西,直罗组下段铀储层砂体非均质性增强,具体表现为砂体厚度明显减薄、含砂率降低,泥岩层数量和厚度均显著增加,内部开始发育薄层煤线。这种组合的出现在大营西侧形成了规模较大的横向泥质隔挡层和垂向还原层,在后期成矿过程中极大地抑制了层间氧化带向西推进的速率和里程,从而在大营一带形成稳定的层间氧化带前锋线和持续的铀矿化,这很可能是造就大营—塔然高勒—纳岭沟一带铀超常富集的主控因素之一。

(3)铀矿化体三维属性模型显示,大营弧形展布的铀矿化体与东部相邻的纳岭沟—塔然高勒铀矿化几乎相连、相通,且两矿床之间亦有较强的放射性异常显示,指示着大营与纳岭沟之间的塔然高勒—乌定布拉格一带具有相似的成矿条件并具有很好的找矿潜力。

**致谢**:中国地质大学(武汉)吴立群副教授及孙钰函博士、内蒙古地质调查院杨才教授级高级工程师等人一起参加了三维地质建模工作;中国地质调查局天津地质调查中心李承东研究员、赵凤清研究员给予了诸多宝贵建议,在此一并致谢。

## References

Courrioux G, Nullans S, Guillen A. 2001. 3DVolumetric modelling of Cadomian Terranes (Northern Brittany, France): An automatic method using vorono diagrams[J]. Tectonophysics, 331(1/2): 181−196.

Cui Tingzhu, Ma Xueping. 2010. An application of 3d structural modeling to complex fault − block reservoirs − A case of the lower unit reservoir of sha−3 member in block Wei−95, Mazhai oil field, Dongpu depression[J]. Oil & Gasgeology, 31(2): 198− 205 (in Chinese with English abstract).

Chen Chao, Chen Guofeng. 2012. Application and research of three dimensional modeling in district geologic survey[J]. City Geology, 7(1): 20−25 (in Chinese with English abstract).

Chen Yingjun, Yan Jiayong. 2014. Progress and examples of three−dimensional geological mapping in Australia[J]. Geology and Exploration, 50(5): 884−892 ( in Chinese with English abstract).

Chen Yin, Feng Xiaoxi, Chen Lulu, Jin Ruoshi, Miao Peisen, Sima Xianzhang, Miao Aisheng, Tang Chao, Wang Gui, Liu Zhongren. 2017. An analysis of U−Pb dating of detrital zircons and modes of occurrence of uranium minerals in the Zhiluo Formation of northeastern Ordos Basin and their indication to uranium sources[J]. Geology in China, 44(6): 1190−1206 (in Chinese with English abstract).

Feng Xiaoxi, Teng Xueming, He Youyu. 2019. Study on land subsidence assessment in evaluation of carrying capacity of geological environment[J]. Geological Survey and Research, 42(2): 96−108 (in Chinese with English abstract).

Guiziou J L, Mallet J L, Madariaga R. 1996. 3D seismic reflection tomography on top of the gocad depth modeler[J]. Geophysics,61 (5): 1499−1510.

Jachens R C, Wentworth C M, Gautier D L. 2001. 3D Geologic Maps and Visualization: A New Approach to the Geology of the Santa Clara (Silicon Valley), California[J]. Digital Mapping Techniques 01, U.S. Geological Survey Open−File Report 1−223, 13−23.

Jiao Yangquan, Wu Liqun, Yang Shengke, Lü Xinbiao, Yang Qin, Wang Zhenghai, Wang Minfang. 2006. Sedimentology of Uranium Reservior: The Exploration and Development Base of Sandstone−Type Uranium Deposits[M]. Beijing: Geological Publishing House, 1−323 ( in Chinese).

Jiao Yangquan, Wu Liqun, Rong Hui, Peng Yunbiao, Wan Junwei, Miao Aisheng. 2012. Uranium reservoir architecture and ore−forming flow field study: A key of revealing Dongsheng sandstone− type uranium deposit mineralization mechanism[J]. Geological Science and Technology Information, 31(5): 94− 104 (in Chinese with English abstract).

Jiao Yangquan, Wu Liqun, Peng Yunbiao, Rong Hui, Ji Dongmin, Miao Aisheng, Li Hongliang. 2015. Sedimentary− tectonic setting of the deposition− type uranium deposits forming in the Paleo−Asian tectonic domain, North China[J]. Earth Science Frontiers, 22 (1): 189−205 (in Chinese with English abstract).

Jiao Y Q, Wu L Q, Rong H .2016. The relationship between Jurassic coal measures and sandstone− type uranium deposits in the northeastern Ordos Basin, China[J]. Acta Geologica Sinica, 90(6): 2117 −2132.

Jiao Yangquan, Wu Liqun1, Rong Hui, Zhang Fan, Yue Liang, Tao Zhenpeng, Sun Yuhan. 2018. Geological modeling of uranium reservoir: The geological foundation of revealing the metallogenic mechanism and solving“remaining uranium”[J]. Earth Science, 43 (10): 3568−3583 (in Chinese with English abstract).

Jin Ruoshi, Cheng Yinhang, Li Jianguo, Sima Xianzhang, Miao Peisen, Wang Shaoyi, Ao Cong, Li Hongliang, Li Yangfeng, Zhang Tianfu. 2017. Late Mesozoic continental basin “Red and Black beds” coupling formation constraints on the sandstone uranium mineralization in northern China[J]. Geology in China, 44(2): 205−223 (in Chinese with English abstract).

Jin Ruoshi, Yu Rengan, Yang Jun, Zhou Xiaoxi, Teng Xueming, Wang Shanbo, Si Qinghong, Zhu Qiang and Zhang Tianfu. 2019. Paleo−environmental constraints on uranium mineralization in the Ordos Basin: Evidence from the color zoning of U−bearing rock series[J]. Ore Geol. Rev., 104: 175−189.

Jin Ruoshi, Teng Xueming, Li Xiaoguang, Si Qinghong, Wang Wei. 2020. Genesis of sandstone− type uranium deposits along the northern margin of the Ordos Basin, China[J]. Geoscience Frontiers, 11(1): 216−228.

Liu Chiyang, Zhao Hongge, Gui Xiaojun, Yue Leping , Zhao Junfeng, Wang Jianqiang. 2006. Space−time coordinate of the evolution and reformation and mineralization response in Ordos Basin[J]. Acta Geologica Sinica, 80(5): 617− 638 (in Chinese with English abstract).

Liu Xiaoxue, Tang Chao, Sima Xianzhang, Zhu Qiang, Li Guangyao, Chen Yin, Chen Lulu. 2016. Major elements geochemical characteristics of sandstone− type uranium deposit in north− east Ordos basin and its geological implactions[J]. Geological Survey and Research, 39(3): 169−176 (in Chinese with English abstract).

Li Sitian, Cheng Shoutian, Yang Shigong, Huang Qisheng, Xie Xinong, Jiao Yangquan, Lu Zongsheng, Zhao Genrong. 1990. Sequence Stratigraphy and Depositional System Analysis of the Northeastern Ordos Basin[M]. Beijing: Geological Publishing House: 1−194 (in Chinese).

Li Sitian, Yang Shouguang, Tomasz J. 1995. Upper Triassic− Jurassic foreland sequences of the Ordos Basin in China stratigraphic, evolution of foreland basins[J]. SEPM Special Publication, 52: 233−241.

Li Qingyuan, Jia Huiling, Wang Baolong, Dong Qianlin, Song Bonian, Wei Xinyong. 2017. 3D geological modeling usage, status quo, existing problems and suggestions[J]. Coal Geology of China, 27 (11): 74−78 (in Chinese with English abstract).

Lu Chao, Jiao Yangquan, Peng Yunbiao, Wu Liqun, Miao Aisheng, Rong Hui, Xie Huili. 2018. Paleo− interlayer oxidation zone identification and spatial localization prediction in Daying area[J]. Geology in China, 45(6): 1228− 1240 (in Chinese with English abstract).

Malolepszy Z. 2005. Three− dimensional geological maps[C]// Ostaficzuk S R.(ed.). The Current Roleof Geological Mapping in Geosciences. NATO Science Series, 56: 215−224.

Mallet J L. 2008. Numerical Earth Models[M]. Nertherland: EAGE Publications:1−144.

Mao Xiancheng, Zou Yanhong, Chen Jin, Lai Jianqing, Peng Shenglin,

Shao Yongjun, Shu Zhiming, Lü Junwu, Lü Caiyu. 2010. Three－dimensional visual prediction of concealed ore bodies in the deep and marginal parts of crisis mines: A case study of the Feng Huangshan ore field in Tongling. Anhui, China[J]. Geological Bulletin of China, 29 (2/3): 401－413 (in Chinese with English abstract).

Miao Peisen, Li Jinguo, Tang Chao, Jin Ruoshi, Cheng Yinhang, Zhao Long, Xiao Peng, Wei Jialin. 2017. Metallogenic condition and prospecting orientation for deep sandstone－ hosted uranium deposits in Mesozoic－ Cenozoic basins of North China[J]. Geological Bulletin of China, 36(10): 1830－1840 (in Chinese with English abstract).

Shao Yanlin, He Youbin, Xu Xiaohong. 2012. Structural modeling under complicated geological features－ by taking Dalinghe oil formation in shu II district as an example[J]. Journal of Oil and Gas Technology, 34 (2): 50 －52 (in Chinese with English abstract).

Wang Xin, Li Ling, Yu Yan, Lu Yonghe, Qu Weiyu, Wang Xueping. 2013. Study on paleogeomorphic restoring and structural development history of Wulanhua Sag, Erlian Basin[J]. China Petroleum Exploration, 18(6): 6－ 68 (in Chinese with English abstract).

Wu Chonglong, Liu Gang. 2015. Current situation, existent problems, trend and strategy of the construction of “Glass Earth” [J]. Geological Bulletin of China, 34(7): 1280－1287( in Chinese with English abstract).

Xiang Zhonglin, Wang Yan, Wang Runhuai, Liu Yufang, Liu Shunxi. 2009. 3D geological modeling and visualization process of minies based on bore hole data[J]. Geological Survey and Research, 45(1): 75－81 (in Chinese with English abstract).

Yu Junjian, Wang Guocan, Xu Yixian, Guo Jisheng, Chen Xujun, Yang Wei, Gong Yiming, Chen Chao, Li Yongtao, Yan Wenbo, Xiao Long. 2015. Constraining deep geological structures in three－dimensional geological mapping of complicated orogenic belts: A case study from Karamay Region, Western Jungga[J]. Earth Science－ Journal of China University of Geoscience,40(3): 407－418 (in Chinese with English abstract).

Yang Junjie, Pei Xigu. 1996. Naturalgas Geology in China[M]. Beijing: Petroleum Industry Press, 3－20 (in Chinese).

Yu Reng'an, Sima Xianzhang, Jin Ruoshi, Miao Peisen, Peng Shenglong. 2020. The new discovery of the Large－scale uranium deposit in the Northeast Ordos Basin[J]. Geology in China, 47(3): 883－884(in Chinese with English abstract).

Zhang Tianfu, Sun Lixin, Zhang Yun , Cheng Yinhang , Li Yanfeng , Ma Haili, Lu Chao, Yang Cai, Guo Genwan. 2016. Geochemical characteristics and paleoenvironmental implications of Jurassic Yan, an & Zhiluo Formation, northern margin of Ordos basin[J]. Acta Geologica Sinica, 90(12): 3454－ 3472 (in Chinese with English abstract).

Zhang Tianfu, Zhang Yun, Miao Peisen, Yu Reng an, Li Jianguo , Jin Ruoshi. 2018. Study on the chemical index of alteration of the Middle and Late Jurassic Strata in the western margin of Ordos basin and its implications[J]. Geological Survey and Research, 41 (4): 258－279 (in Chinese with English abstract).

Zhang Tianfu, Zhang Yun, Cheng Yinhang, Miao Peisen, Ao Cong, Jin Ruoshi, Duan Lianfeng, Duan Xiaolong. 2019. Integrated identification of sequence boundary through outcrop, seismic, logging and geochemistry: A case of Jurassic, the northeastern margin of Ordos basin[J]. Coal Geology & Exploration,47(1): 40－48 (in Chinese with English abstract).

Zhang Tianfu, Zhang Yun, Jin Ruoshi, Yu Reng'an, Sun Lixin, Cheng Yinhang, Ao Cong, Ma Hailin. 2020. Characteristics of Jurassic sequence boundary surfaces on the northeastern margin of Ordos basin and their constraints on the spatial－ temporal properties of sandstone uranium mineralization[J]. Geology in China, 47(2): 278－299(in Chinese with English abstract).

Zhang Yun, Sun Lixin, Zhang Tianfu, Ma Haili, Lu Chao, Li Yanfeng, Cheng Yinhang, Yang Cai, Guo Jiacheng, Zhou Xiaoguang. 2016. The study on sequence stratigraphy of coal－ uranium bearing measures and occurrence regularity of coal－ uranium in northeastern Ordos Basin[J]. Acta Geologica Sinica, 90(12): 3424－3440 (in Chinese with English abstract).

Zhu Liangfeng, Wu Caixin, Liu Xiuguo. 2004. Preliminary study of 3D urban geological information system[J].Geography and Geo－Information Science, 20(5): 36－ 40 (in Chinese with English abstract).

Zhou Xiaoxi, Chen Anshu, Deng Fan, Yang Jun, Wang Xinhua. 2016. Design and realization of uranium mine drilling database of the important basins in North China[J]. Geological Survey and Research, 39(3): 231－236 (in Chinese with English abstract).

## 附中文参考文献

陈超, 陈广峰. 2012. 三维建模技术在区域工程地质勘查中的应用研究[J]. 城市地质, 7(1): 20－25.

陈应军, 严加永. 2014. 澳大利亚三维地质填图进展与实例[J]. 地质与勘探, 50(5): 884－892.

陈印, 冯晓曦, 陈路路, 金若时, 苗培森, 司马献章, 苗爱生, 汤超, 王贵, 刘忠仁. 2017. 鄂尔多斯盆地东北部直罗组内碎屑锆石和铀矿物赋存形式简析及其对铀源的指示[J]. 中国地质, 44(6): 1190－1206.

崔廷主, 马学萍. 2010. 三维构造建模在复杂断块油藏中的应用——以东濮凹陷马寨油田卫95块油藏为例[J]. 石油与天然气地质, 31 (2) : 198－250.

冯晓曦, 滕雪明, 何友宇. 2019. 初步探讨鄂尔多斯盆地东胜铀矿田成矿作用研究若干问题[J]. 地质调查与研究, 42(2): 96－108.

焦养泉, 吴立群, 杨生科, 吕新彪, 杨琴, 王正海, 王敏芳. 2006. 铀储层沉积学: 砂岩型铀矿勘查与开发的基础[M]. 北京: 地质出版社, 1－323.

焦养泉, 吴立群, 荣辉, 彭云彪, 万军伟, 苗爱生. 2012. 铀储层结构与

成矿流场研究: 揭示东胜砂岩型铀矿床成矿机理的一把钥匙[J]. 地质科技情报, 31(5): 94−104.

焦养泉, 吴立群, 彭云彪, 荣辉, 季东民, 苗爱生, 里宏亮. 2015. 中国北方古亚洲构造域中沉积型铀矿形成发育的沉积−构造背景综合分析[J]. 地学前缘, 22(1): 189−205.

焦养泉, 吴立群, 荣辉, 张凡, 乐亮, 陶振鹏, 孙钰函. 2018. 铀储层地质建模: 揭示成矿机理和应对“剩余铀”的地质基础[J]. 地球科学, 43(10): 3568−3583.

金若时, 程银行, 李建国, 司马献章, 苗培森, 王少轶, 奥琮, 里宏亮, 李艳锋, 张天福. 2017. 中国北方晚中生代陆相盆地红−黑岩系耦合产出对砂岩型铀矿成矿环境的制约[J]. 中国地质, 44(2): 205−223.

刘池洋, 赵红格, 桂小军, 岳乐平, 赵俊峰, 王建强. 2006. 鄂尔多斯盆地演化−改造的时空坐标及其成藏(矿)响应[J]. 地质学报, 80(5): 617−638.

刘晓雪, 汤超, 司马献章, 朱强, 李光耀, 陈印, 陈路路. 2016. 鄂尔多斯盆地东北部砂岩型铀矿常量元素地球化学特征及地质意义[J]. 地质调查与研究, 39(3): 169−176.

李思田, 程守田, 杨士恭, 黄其胜, 解习农, 焦养泉, 卢宗盛, 赵根榕. 1990. 鄂尔多斯盆地东北部层序地层及沉积体系[M]. 北京: 地质出版社, 1−194.

李青元, 贾慧玲, 王宝龙, 董前林, 宋博辇, 魏新永. 2016. 三维地质建模的用途、现状、存在问题与建议[J]. 中国煤炭地质, 27(11): 74−78.

鲁超, 焦养泉, 彭云彪, 吴立群, 苗爱生, 荣辉, 谢惠丽. 2018. 大营地区古层间氧化带识别与空间定位预测[J]. 中国地质, 45(6): 1228−1240.

苗培森, 李建国, 汤超, 金若时, 程银行, 赵龙, 肖鹏, 魏佳林. 2017. 中国北方中新生代盆地深部砂岩铀矿成矿条件与找矿方向[J]. 地质通报, 36(10): 1830−1840.

毛先成, 邹艳红, 陈进, 赖健清, 彭省临, 邵拥军, 疏志明, 吕俊武, 吕才玉. 2010. 危机矿山深部,边部隐伏矿体的三维可视化预测——以安徽铜陵凤凰山矿田为例[J]. 地质通报, 29 (2/3):401−413.

邵燕林, 何幼斌, 许晓宏. 2012. 复杂地质特征下的构造建模——以辽河油田曙二区大凌河油层为例[J]. 石油天然气学报, 34 (2): 50−52.

王鑫, 李玲, 余雁, 卢永合, 屈伟玉, 王雪萍. 2013. 二连盆地乌兰花凹陷古地貌恢复及构造发育史研究[J]. 中国石油勘探, 18(6): 6−68.

吴冲龙, 刘刚. 2015. “玻璃地球”建设的现状、问题、趋势与对策[J]. 地质通报, 34(7): 1280−1287.

向中林, 王妍, 王润怀, 刘玉芳, 刘顺喜. 2009. 基于钻孔数据的矿山三维地质建模及可视化过程研究[J]. 地质调查与研究, 45(1): 75−81.

郁军建, 王国灿, 徐义贤, 郭纪盛, 陈旭军, 杨维, 龚一鸣, 陈超, 李永涛, 晏文博, 肖龙. 2015. 复杂造山带地区三维地质填图中深部地质结构的约束方法——西准噶尔克拉玛依后山地区三维地质填图实践[J]. 地球科学——中国地质大学学报, 40(3): 407−418.

杨俊杰, 裴锡古. 1996. 中国天然气地质学[M]. 北京: 石油工业出版社, 3−20.

俞礽安, 司马献章, 金若时, 苗培森, 彭胜龙. 2020. 鄂尔多斯盆地东北缘发现大型砂岩型铀矿床[J]. 中国地质, 47(3): 883−884.

张天福, 孙立新, 张云, 程银行, 李艳峰, 马海林, 鲁超, 杨才, 郭根万. 2016. 鄂尔多斯盆地北缘侏罗纪延安组、直罗组泥岩微量元素、稀土元素地球化学特征及其古沉积环境意义[J]. 地质学报, 90(12): 3454−3472.

张天福, 张云, 苗培森, 俞礽安, 李建国, 金若时, 孙立新. 2018. 鄂尔多斯盆地西缘中晚侏罗世地层化学蚀变指数(CIA)研究及其意义[J]. 地质调查与研究, 41(4): 258−262.

张天福, 张云, 程银行, 苗培森, 奥琮, 金若时, 段连峰, 段霄龙. 2019. 利用露头、井震及地球化学综合厘定层序界面——以鄂尔多斯盆地东北缘侏罗系为例[J]. 煤田地质与勘探, 47(1): 40−48.

张天福, 张云, 金若时, 俞礽安, 孙立新, 程银行, 奥琮, 马海林. 2020. 鄂尔多斯盆地东北缘侏罗系层序界面特征对砂岩型铀矿成矿环境的制约[J]. 中国地质, 47(2): 278−299.

张云, 孙立新, 张天福, 马海林, 鲁超, 李艳峰, 程银行, 杨才, 郭佳城, 周晓光. 2016. 鄂尔多斯盆地东北缘煤铀岩系层序地层与煤铀赋存规律研究[J]. 地质学报, 90(12): 3424−3440.

朱良峰, 吴信才, 刘修国. 2004. 城市三维地质信息系统初探[J]. 地理与地理信息科学, 20(5): 36−40.

周小希, 陈安蜀, 邓凡, 杨君, 王心华. 2016. 北方重要盆地铀矿钻孔数据库设计及实现[J]. 地质调查与研究, 39(3): 231−236.